

Constrained Deformation of a Confined Solid: Anomalous Failure by Nucleation of Smectic Bands

Debasish Chaudhuri and Surajit Sengupta

Satyendra Nath Bose National Centre for Basic Sciences, Block-JD, Sector-III, Salt Lake, Calcutta - 700098, India

(Received 8 January 2004; published 9 September 2004)

We report results of computer simulations of the deformation and failure behavior of a thin crystalline strip of “hard disks” in two dimensions confined within a quasi-one-dimensional “hard-wall” channel of fixed width corresponding to a few disk diameters. Starting from a commensurate triangular solid, stretching the strip along its length introduces a rectangular distortion. This, beyond a critical strain, leads to failure of the solid by “phase separation” into alternating bands of solid and *smectic*-like phases. The critical strain is *inversely* proportional to the channel width, i.e., thinner strips are stronger. The large plastic deformation which precedes failure is observed to be reversible.

DOI: 10.1103/PhysRevLett.93.115702

PACS numbers: 64.60.Cn, 61.30.-v, 62.25.+g, 68.08.-p

Studies of small assemblages of molecules with one or more dimensions comparable to a few atomic spacings are significant in the context of nanotechnology [1]. Designing nanosized machines requires a knowledge of the mechanical behavior of systems up to atomic scales, where, *a priori*, there is no reason for our ideas, derived from macroscopic continuum elasticity theory, to be valid [2]. Small systems often show entirely new behavior if hard constraints are imposed leading to confinement in one or more directions. Consider, for example, the rich phase behavior of quasi-two-dimensional colloidal solids [3,4] confined between two glass plates showing square, triangular, and “buckled” crystalline phases and a recently observed reentrant surface melting transition [5] of colloidal hard spheres not observed in the bulk [6–8].

A bulk solid, strained beyond its critical limit, fails by the nucleation and growth of cracks [9–11]. The interaction of dislocations or zones of plastic deformation [10,12] with the growing crack tip determines the failure mechanism, viz., either ductile or brittle fracture. Studies of the fracture of single-walled carbon nanotubes [13] also show failure driven by bond-breaking which produces nanocracks which run along the tube circumference leading to brittle fracture. Thin nanowires of Ni are known [14], on the other hand, to show ductile failure with extensive plastic flow and amorphization. In general, nanostructured materials are known [15] to have superior fracture resistance.

In this Letter, we investigate the failure, under tension, of a confined solid, composed of atoms interacting by purely entropic forces, in quasi-one-dimension. We perform computer simulations, in the constant number and strain ensemble, of two-dimensional hard disk “atoms” confined within a long one-dimensional channel, just wide enough to accommodate only a few (n_l) atomic layers of a defect free triangular lattice. Unlike bulk solids, nanotubes, or wires, we find that failure in this case is *not* mediated by cracks but commences by the

generation of bands of a $n_l - 1$ layered *smectic* phase [16] within the solid as the length of the system is increased (Fig. 1). Nevertheless, the critical strain for failure by this novel mechanism, for small $n_l < 25$, increases with decreasing channel width. Thinner strips are *more* resistant to failure due to a kinetic hindrance to the creation of dislocation pairs. Fracture is ductile, with large prefailure plastic deformation which is reversible, i.e., the stress-strain curve is traced back (see Fig. 2) once the sense of strain is reversed. Our results may be directly verified in experiments on sterically stabilized “hard sphere” colloids [17] confined in glass channels. Some aspects of our results may also be relevant for similarly confined atomic systems interacting with more complex potentials.

The bulk system of hard disks where particles i and j , in two dimensions, interact with the potential $V_{ij} = 0$ for

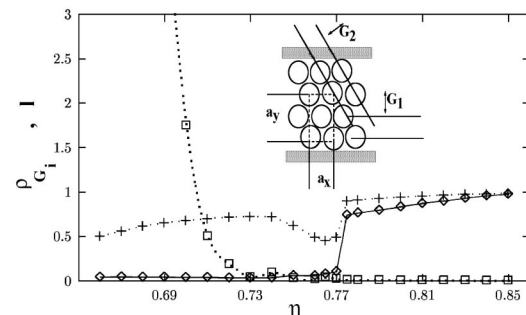


FIG. 1. Results of canonical ensemble Monte Carlo (MC) simulations of $N = 65 \times 10$ hard disks confined between two parallel hard walls separated by a distance $L_y = 9d$. For each η , the system was equilibrated over 10^6 MC steps (MCS) and data averaged over a further 10^6 MCS. At $\eta = 0.85$, we have a strain-free triangular lattice. Plots show the structure factors $\rho_{\mathbf{G}_i}$, $i = 1(+), 2(\diamond)$ for RLVs $\mathbf{G}_i(\eta)$, averaged over symmetry related directions, as a function of η and the Lindemann parameter $l(\square)$. The lines in the figure are a guide to the eye. Inset shows the geometry used, the reciprocal lattice vectors (RLVs) \mathbf{G}_1 and \mathbf{G}_2 , and the rectangular unit cell.

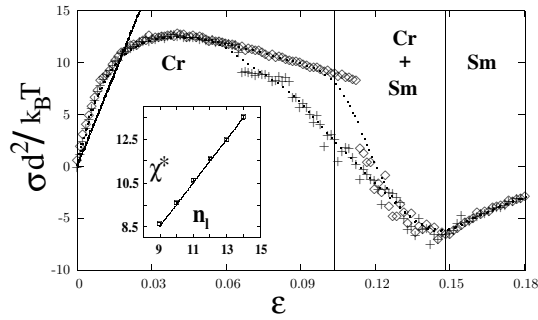


FIG. 2. A plot of the conjugate stress σ versus external strain ϵ obtained from MC simulations of 65×10 hard disks initially at $\eta = 0.85$. Regions corresponding to a crystal (Cr), smectic (Sm), and the mixed phase are marked. Data is obtained after equilibrating at each strain value for 2×10^4 MCS and averaging over a further 3×10^4 MCS. The dotted lines are a guide to the eye and the solid straight line is the prediction of free volume theory (see text), which slightly underestimates the elastic constant. The entire cycle of increasing ϵ (\diamond) and decreasing to zero (+) using typical parameters appropriate for an atomic system corresponds to a real frequency of $\omega \approx 100$ KHz. Results do not essentially change for $\omega = 10$ KHz – 1 MHz. Inset shows the variation of the critical χ^* with n_l , points: simulation data; line: $\chi^* = n_l - 1/2$.

$|\mathbf{r}_{ij}| > d$ and $V_{ij} = \infty$ for $|\mathbf{r}_{ij}| \leq d$, where d is the hard disk diameter and $\mathbf{r}_{ij} = \mathbf{r}_j - \mathbf{r}_i$, the relative position vector of the particles, has been extensively [6–8] studied. Apart from being easily accessible to theoretical treatment [18], experimental systems with nearly “hard” interactions, viz., sterically stabilized colloids [17] are available. The hard disk free energy is entirely entropic in origin and the only thermodynamically relevant variable is the number density $\rho = N/V$ or the packing fraction $\eta = (\pi/4)\rho d^2$ the energy scale being set by $k_B T$. Accurate computer simulations [7] of hard disks show that for $\eta > \eta_f = 0.719$ the system exists as a triangular lattice which melts below $\eta_m = 0.706$. Elastic constants of bulk hard disks have been calculated in simulations [8,19]. The surface free energy of the hard disk system in contact with a hard-wall has also been obtained [20] taking care that the dimensions of the system are compatible with a strain-free triangular lattice.

Consider a narrow channel in two dimensions of width L_y defined by hard walls at $y = 0$ and L_y ($V_{\text{wall}}(y) = 0$ for $d/2 < y < L_y - d/2$ and $= \infty$ otherwise) and length L_x with $L_x \gg L_y$. Periodic boundary conditions are assumed in the x direction. In contrast to the quasi-two-dimensional case studied in Refs. [3,4], the reduced dimensionality severely limits the choice of available structures. Within the extensive parameter range explored by us, we do not find evidence for a stable homogeneous structure that continuously interpolates between a n_l and $n_l \pm 1$ layered triangular lattice analogous to the buckled phase [3,4]. Therefore, in order that the channel

may accommodate n_l layers of a homogeneous triangular lattice with lattice parameter a_0 of hard disks of diameter d , (Fig. 1) one needs

$$L_y = \frac{\sqrt{3}}{2}(n_l - 1)a_0 + d, \quad (1)$$

with $L_x = n_x a_0$, where n_x is the number of unit cells in the x - direction. For a system of constant number of particles ($N = n_x n_l$) and L_y , a_0 is decided by $\eta = \pi N d^2 / 4 L_x L_y$. Defining $\chi(\eta, L_y) = 1 + 2(L_y - d) / \sqrt{3} a_0$, Eq. (1) reads $\chi = \text{integer} = n_l$ and violation of Eq. (1) implies a rectangular strain away from the reference triangular lattice of n_l layers. The lattice parameters of a centered rectangular (CR) unit cell are a_x and a_y (Fig. 1 inset). In general, for a CR lattice with given L_y we have $a_y = 2(L_y - d) / (n_l - 1)$ and, ignoring vacancies, $a_x = 2 / \rho a_y$.

Calculation of the deformation strain needs some care at this stage. Using the initial triangular solid (packing fraction η_0) as reference, the “external” strain associated with changing L_x , while keeping L_y fixed, is $\epsilon = (\eta_0 - \eta) / \eta$ where η is the packing fraction of the deformed solid. Internally, the solid is, however, free to adjust n_l to decrease its energy (strain). Therefore, one needs to calculate strains with respect to a reference, distortion-free, triangular lattice at η . Using the definition $\epsilon_d = \epsilon_{xx} - \epsilon_{yy} = (a_x - a_0) / a_0 - (a_y - \sqrt{3} a_0) / \sqrt{3} a_0$ and the expressions for a_x , a_y , and a_0 given above, we get

$$\epsilon_d = \frac{n_l - 1}{\chi - 1} - \frac{\chi - 1}{n_l - 1}, \quad (2)$$

where the number of layers n_l is the nearest integer to χ so that ϵ_d has a discontinuity at half-integral values of χ . For large L_y , this discontinuity and ϵ_d itself vanishes as $1/L_y$ for all η . This “internal” strain ϵ_d is related nonlinearly to ϵ and may remain small even if ϵ is large. Note that any pair of variables η and L_y (or alternately ϵ and χ) uniquely fixes the state of the system.

We study the effects of strain on the hard disk triangular solid at fixed L_y large enough to accommodate a small number of layers $n_l \sim 9 - 25$. We monitor the Lindemann parameter $l = \langle (u_i^x - u_j^x)^2 \rangle / a_x^2 + \langle (u_i^y - u_j^y)^2 \rangle / a_y^2$ where the angular brackets denote averages over configurations, i and j are nearest neighbors, and u_i^α is the α th component of the displacement of particle i from its mean position. The parameter l diverges at the melting transition [21]. We also measure the structure factor $\rho_{\mathbf{G}} = |\langle \frac{1}{N} \sum_{j,k=1}^N \exp(-i\mathbf{G} \cdot \mathbf{r}_{jk}) \rangle|$ for $\mathbf{G} = \pm \mathbf{G}_1(\eta)$, the reciprocal lattice vector (RLV) corresponding to the set of close-packed lattice planes of the CR lattice perpendicular to the wall, and $\pm \mathbf{G}_2(\eta)$ the four equivalent RLVs for close-packed planes at an angle ($= \pi/3$ and $2\pi/3$ in the triangular lattice) to the wall (see Fig. 1 inset).

Throughout, $\rho_{G_2} < \rho_{G_1} \neq 0$, a consequence of the hard-wall constraint [20] which manifests as an oblate anisotropy of the local density peaks in the solid. As η is decreased, both ρ_{G_1} and ρ_{G_2} show a jump at $\eta = \eta_{c_1}$ where $\chi = \chi^* \approx n_l - 1/2$ (Fig. 2 inset). For $\eta < \eta_{c_1}$, we get $\rho_{G_2} = 0$ with $\rho_{G_1} \neq 0$, signifying a transition from crystalline to smectic-like order. The Lindemann parameter l remains zero and diverges only below $\eta = \eta_{c_3} (\approx \eta_m)$, indicating a finite-size broadened melting of the smectic to a modulated liquid phase. The stress [22], $\sigma = \sigma_{xx} - \sigma_{yy}$ in units of $k_B T/d^2$, versus strain, ϵ , curve is shown in Fig. 2. For $\eta = \eta_0$ ($\epsilon = 0$) the stress is purely hydrostatic with $\sigma_{xx} = \sigma_{yy}$ as expected. Initially, the stress increases linearly, flattening out at the onset of plastic behavior at $\eta \leq \eta_{c_1}$. At η_{c_1} , with the nucleation of smectic bands, σ decreases and eventually becomes negative. At η_{c_2} , the smectic phase spans the entire system and σ is minimum. On further decrease in η towards η_{c_3} , σ approaches zero from below (Fig. 2), thus forming a van der Waals loop. If the strain is reversed by increasing η back to η_0 , the entire stress-strain curve is traced back with no remnant stress at $\eta = \eta_0$ showing that the plastic region is reversible. For the system shown in Figs. 1 and 2, we obtained $\eta_{c_1} \approx 0.77$, $\eta_{c_2} \approx 0.74$, and $\eta_{c_3} \approx 0.7$. As L_y is increased, η_{c_1} merges with η_{c_3} for $n_l \geq 25$. If instead, L_x and L_y are both rescaled to keep $\chi = n_l$ fixed or periodic boundary conditions are imposed in both x and y directions, the transitions in the various quantities occur approximately simultaneously as expected in the bulk system. Varying n_x in the range 10–1000 produces no essential change in results.

For $\eta_{c_2} < \eta < \eta_{c_1}$, we observe that the smectic order appears within narrow bands (Fig. 3). Inside these bands, the number of layers is less by one and the system in this range of η is in a mixed phase. A plot [Fig. 3(a) and 3(b)] of $\chi(x, t)$, where we treat χ as a space and time (MCS) dependent “order parameter” (configuration averaged number of layers over a window in x and t), shows bands

in which χ is less by one compared to the crystalline regions. Once nucleated narrow bands coalesce to form wider bands, the dynamics of which is, however, extremely slow. The total size of such bands grows as η is decreased. Calculated diffraction patterns [Fig. 3(c) and 3(d)] show that, locally, within a smectic band $\rho_{G_1} \gg \rho_{G_2}$ in contrast to the solid region where $\rho_{G_1} \approx \rho_{G_2} \neq 0$.

The total free energy per unit volume of a *homogeneous* solid, \mathcal{F}^T , which is in contact with a hard-wall and distorted with a (small) strain ϵ_d is given by

$$\mathcal{F}^T(\eta, \chi) = \frac{1}{2} K^\Delta(\eta) \epsilon_d^2(\chi) + \mathcal{F}^\Delta(\eta), \quad (3)$$

where $K^\Delta(\eta)$ is an elastic constant and $\mathcal{F}^\Delta(\eta)$ the free energy of the (undistorted) triangular lattice in contact with a hard-wall [20] at packing fraction η . The “fixed neighbor” free volume $v_f(\eta, \epsilon_d)$ may be obtained using straight forward, though rather tedious, geometrical considerations [20] so that $\mathcal{F}^\Delta(\eta) = -\rho \log v_f(\eta, 0)$ and $K^\Delta(\eta) = \partial^2 \mathcal{F}^\Delta(\eta, \epsilon_d) / \partial \epsilon_d^2 |_{\epsilon_d=0}$ (see Fig. 2). It is clear that \mathcal{F}^T has minima for all $\chi = n_l$. For half-integral values of χ , the homogeneous crystal is locally unstable. Noting that $\chi^* = n_l - 1/2$ (Fig. 2 inset), it follows from Eq. (2) the critical strain $\epsilon_d^* = (4n_l - 5)/(2n_l - 3)(2n_l - 2) \sim 1/n_l$ which is supported by our simulation data over the range $9 < n_l < 14$. At these strains, the solid generates bands consisting of regions with one less atomic layer. Within these bands, adjacent local density peaks of the “atom’s overlap in the x direction producing a smectic. Indeed, the overlap $\sqrt{\langle u_x^2 \rangle} / a_x$ maybe calculated using simple density functional arguments [23] to be $(\chi - 1)/4\pi\sqrt{C_0\rho_{G_2}}(n_l - 1)$ (where C_0 is a constant of order unity) which, evidently, diverges as $\rho_{G_2} \rightarrow 0$. For large L_y , the minima in \mathcal{F}^T merge to produce a smooth free energy surface independent of χ and more conventional modes of failure, viz., cracks, are expected to become operative.

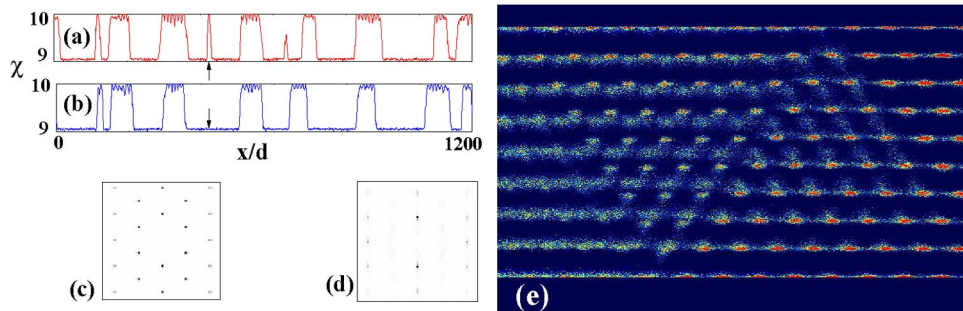


FIG. 3 (color online). Plot of $\chi(x, t)$ as a function of the x/d at $\eta = 0.76$ after time $t =$ (a) 5×10^5 and (b) 2×10^6 MCS for $N = 10^3 \times 10$. Note that $\chi = 10$ in the solid and $\chi = 9$ in the smectic regions. Arrows show the coalescence of two bands as a function of time. Calculated diffraction patterns for the (c) solid and (d) smectic regions. (e) Close-up view of a crystal-smectic interface from superimposed positions of 10^3 configurations at $\eta = 0.77$. The colors code the local density of points from red/dark (high) to blue/light (low). Note the misfit dislocation in the interfacial region.

For small L_y , all regions of the parameter space corresponding to nonintegral χ are also *globally* unstable as belied by the loop in the stress-strain curve (Fig. 2). The system should therefore break up into regions with n_l and $n_l - 1$ layers for very small ε_d . Such fluctuations are, however, kinetically suppressed, as we argue below, making thin strips resistant to failure. A superposition of many particle positions near such an interface [see Fig. 3(e)] shows that: (1) the width of the interface is large, spanning about 10–15 atomic spacings and (2) the interface between n_l layered crystal and $n_l - 1$ layered smectic contains a *dislocation*[24] with Burger's vector in the y direction which makes up for the difference in the number of layers. Each band of width s is therefore held in place by a dislocation-antidislocation pair (Fig. 3). In analogy with classical nucleation theory [23,25], the free energy F_b of a single band can be written as

$$F_b = -\Delta F s + E_c + \frac{1}{8\pi} b^2 K \log \frac{s}{a_0}, \quad (4)$$

where $b = a_y/2$ is the Burger's vector, ΔF the free energy difference between the crystal and the smectic per unit length, E_c the core energy for a dislocation pair, and K an elastic constant ($= K^\Delta$ for the perfect triangular lattice). Bands form when dislocation pairs separated by $s > \frac{1}{8\pi} b^2 K / \Delta F$ arise due to random fluctuations. Note that as $\chi \rightarrow \chi^*$, $K \rightarrow 0$, facilitating band nucleation. Using a procedure similar to that used in Ref. [8], we have monitored the dislocation probability as a function of η . Not surprisingly, the probability of obtaining dislocation pairs with the relevant Burger's vector increases dramatically as $\eta \rightarrow \eta_{c_1}$ and artificially removing configurations with such dislocations *suppresses the transition completely*. Band coalescence occurs by a diffusion aided dislocation "climb," which at high density implies slow kinetics. Throughout the two-phase region, the crystal is in compression and the smectic in tension along the y direction so that σ is completely determined by the amount of the coexisting phases, orientation relationships between the two phases being preserved throughout. This, together with the absence of free dislocations in the confined solid, explains the reversible [26] plastic deformation in Fig. 2.

Apart from constrained hard sphere colloids [17] where our results are directly testable, a similar fracture mechanism may be observable in experiments on the deformation of monolayer nanobeams or strips of real materials, provided the confining channel is made of a material which is harder and has a much smaller atomic size than that of the strip [1]. The effect of elasticity and corrugations of the walls on the fracture process, as well as its dynamics, are interesting directions of future study.

The authors thank M. Rao, V. B. Shenoy, A. Chaudhuri, and A. Datta for useful discussions; D. C. thanks C.S.I.R.,

India, for financial support. Financial support from DST Grant No. SP/S2/M-20/2001 is gratefully acknowledged.

-
- [1] R. Giau *et al.*, Phys. Rev. Lett. **85**, 622 (2000); A. N. Cleland and M. L. Roukes, Appl. Phys. Lett. **69**, 2653 (1996).
 - [2] I. Goldhirsh and C. Goldenberg, Eur. Phys. J. E **9**, 245 (2002).
 - [3] S. Naser *et al.* Phys. Rev. Lett. **79**, 2348 (1997).
 - [4] M. Schmidt and H. Lowen, Phys. Rev. Lett. **76**, 4552, (1996); T. Chou and D. R. Nelson, Phys. Rev. E, **48**, 4611 (1993).
 - [5] R. P. A. Dullens and W. K. Kegel, Phys. Rev. Lett. **92**, 195702 (2004).
 - [6] B. J. Alder and T. E. Wainwright, Phys. Rev. **127**, 359 (1962); J. A. Zollweg, G. V. Chester, and P. W. Leung, Phys. Rev. **B39**, 9518 (1989); H. Weber and D. Marx, Europhys. Lett. **27**, 593 (1994).
 - [7] A. Jaster, Physica A (Amsterdam) **277**, 106 (2000).
 - [8] S. Sengupta, P. Nielaba, and K. Binder, Phys. Rev. E **61**, 6294 (2000).
 - [9] J. A. Hauch, D. Holland, M. P. Marder, and H. L. Swinney, Phys. Rev. Lett. **82**, 3823 (1999); D. Holland and M. Marder, Phys. Rev. Lett. **80**, 746 (1998).
 - [10] J. S. Langer, Phys. Rev. E **62**, 1351 (2000).
 - [11] A. A. Griffith, Philos. Trans. R. Soc. London A **221**, 163 (1920).
 - [12] R. Löfstedt, Phys. Rev. E **55**, 6726 (1997).
 - [13] T. Belytschko *et al.*, Phys. Rev. B **65**, 235430 (2002); M. F. Yu *et al.*, Science **287**, 637 (2000).
 - [14] H. Ikeda *et al.*, Phys. Rev. Lett. **82**, 2900 (1999); P. S. Branicio and J.-P. Rino, Phys. Rev. B **62**, 16950 (2000).
 - [15] R. K. Kalia *et al.*, Phys. Rev. Lett. **78**, 2144 (1997).
 - [16] S. Ostlund and B. I. Halperin, Phys. Rev. B **23**, 335 (1981).
 - [17] I. W. Hamley, *Introduction to Soft Matter: Polymer, Colloids, Amphiphiles and Liquid Crystals* (Wiley, Clchester, 2000).
 - [18] J. P. Hansen and I. R. MacDonald, *Theory of Simple Liquids* (Wiley, Clchester, 1989).
 - [19] K. W. Wojciechowski and A. C. Brańka, Phys. Lett. A **134**, 314 (1988).
 - [20] M. Heni and H. Löwen, Phys. Rev. E **60**, 7057 (1999).
 - [21] K. Zahn, R. Lenke and G. Maret, Phys. Rev. Lett. **82**, 2721 (1999).
 - [22] O. Farago and Y. Kantor, Phys. Rev. E **61**, 2478 (2000).
 - [23] P. M. Chaikin and T. C. Lubensky, *Principles of Condensed Matter Physics* (Cambridge University Press, Cambridge, England, 1995).
 - [24] A comparison of Fig. 3(e) with Fig. 1 of Ref. [3] leads us to speculate whether a two-dimensional version of the buckled phase may in fact wet the solid-smectic interface thereby reducing its energy.
 - [25] J. S. Langer in *Solids Far from Equilibrium*, edited by C. Godrèche (Cambridge University Press, Cambridge, England, 1992).
 - [26] For reversible plasticity in smectic vesicles, see T. Roopa and G. V. Shivashankar, Appl. Phys. Lett. **82**, 1631 (2003); T. Roopa *et al.*, report, 2003 (to be published).